On the Nature of the Perforated Layer Phase in Undiluted Diblock Copolymers

Shuyan Qi

Division of Physics, Mathematics, and Astronomy, California Institute of Technology, Pasadena, California 91125

Zhen-Gang Wang*

Division of Chemistry and Chemical Engineering, California Institute of Technology, Pasadena, California 91125

Received February 13, 1997; Revised Manuscript Received May 1, 1997[⊗]

ABSTRACT: The nature, stability, and mechanism of formation of the block copolymer perforated lamellar structure are elucidated. This structure is shown to develop from the anisotropic fluctuations of the lamellar phase when it reaches its spinodal. It is proposed that there can be two different perforated lamellar structures, one based on a hexagonal close packed (hcp) lattice and one based on a body-centered cubic (bcc) lattice, with nearly degenerate free energy. In the framework of a Leibler-type free energy functional, it is shown that the perforated lamellar structure is only pseudostable (corresponding to a saddle point in the free energy surface) in the weak-segregation limit but can become metastable in the intermediate-segregation regime. Calculation of the fluctuation spectrum of metastable perforated lamellar structures enables us to explain in a simple and consistent manner several puzzling structural data from small-angle neutron scattering studies.

I. Introduction

One of the most fascinating properties of block copolymers is their ability to microphase separate into a variety of ordered morphologies. Undiluted diblock copolymers represent the simplest system for studying the various aspects of microphase transitions and hence have been the subject of extensive experimental and theoretical investigations for the past two decades.[1] Earlier theories predicted only three stable ordered phases:[2,3] lamellar (L), hexagonally ordered cylinders (H) and body-centered cubic (bcc) ordered spheres (BCC). More recent experiments have revealed three additional "complex" morphologies: hexagonally modulated layers (HML),[4] hexagonally perforated layers (HPL),[4,5] and the bicontinuous double gyroid (G).[6,7] The structure of the G phase has been well characterized through a combination of X-ray diffraction and transmission electron microscopy (TEM) studies.[6] Also, state-of-the-art mean-field calculations predict that the G phase is stable between the L and H phases, ending at a triple point on the high-temperature end of the phase diagram.[8,9]

The status of the HML and HPL phases is much less satisfactory. From small-angle neutron scattering (SANS) and TEM studies,[4,10,11] it is believed that the HML phase consists of alternating minority and majority component layers in which the thickness of the minority component domains is modulated with a hexagonal in-layer symmetry. In the HPL phase the majority component is envisioned to form hexagonally ordered channels that extend through the minority component and connect the layers formed by the majority component. However, the three-dimensional stacking of the HML modulations and the HPL perforations is still not known, and this lack of structural information has led several theoretical calculations[12−14] to assume different structures, which resulted in conflicting conclusions with regard to their thermodynamic stability.

Of foremost importance in resolving the structural nature of the HML and HPL phases is a consistent interpretation of the SANS data of Bates and coworkers. There are two outstanding puzzles from these scattering data: the in-layer scattering pattern exhibits six weak broad peaks at wavevectors whose magnitudes are slightly less than that corresponding to the reciprocal of the layer spacing,[4] and in samples where the perforations were assumed to be stacked in the *abcabc*... pattern (in order to explain other features of the data), two distinct scattering peaks were missing at positions where they were expected to appear.[10] Bates and coworkers have proposed some rather elaborate structural mechanisms that offer partial explanations for their scattering data, but these two puzzling observations have never been satisfactorily explained.

Recently, using a time-dependent Ginzburg−Landau approach, we have addressed the kinetics of microphase transitions in diblock copolymers.[15,16] In particular, our numerical simulations show that transition from the L phase to the H phase involves intermediate states whose structural features are strongly reminiscent of the HML and HPL phases.[15] Using a multimode analysis under the single wavenumber approximation, we argued that the perforated layer (PL) structure is a saddle point that lies on the pathway between the L and the H phases while the modulated layer (ML) structure is simply the incipient PL and results from the most unstable mode of the L phase when the L phase reaches its spinodal. Since the ML and PL structures do not differ in symmetry but only differ in the degree of density modulation, we shall refer to both as the PL phase in the remainder of this paper. Also, we shall refer to the perforated layers as PL rather than HPL, because we believe that the in-plane structure is not necessarily of hexagonal symmetry. Yeung et al.[17] and Laradji et al.,[18] on the basis of a theory of anisotropic fluctuations in ordered diblock copolymers recently developed by Shi et al.,[19] have also suggested that the modulated or perforated layer states are due to fluctuation modes of the lamellar phase; however, they did not address the three-dimensional structures.

* To whom correspondence should be addressed.
[⊗] Abstract published in *Advance ACS Abstracts,* July 1, 1997.

S0024-9297(97)00206-4 CCC: $14.00

In this paper, we combine ideas in these recent studies to put forth a unified description of the nature, stability, and possible mechanism of formation of the PL structure in undiluted diblock copolymers. Using a simple, Leibler free energy functional, we show that the PL develops from anisotropic fluctuations of the lamellar phase when it reaches its limit of metastability. We propose two different PL structures, one based on a hexagonal close packed (hcp) lattice and one based on a bcc lattice, with nearly degenerate free energies. In the framework of this free energy, we find that the PL structure is pseudostable (corresponding to a saddle point in the free energy surface) in the weak segregation limit but can become metastable in the intermediate-segregation regime. Our proposed structures produce features that are consistent with all known structural data on the PL structure. In particular, by studying the fluctuation spectrum of the metastable PL structures, we are able to explain in a simple and consistent manner the two puzzles mentioned earlier. In addition, our study provides important insights to the experimental conditions that produce the PL structures.

II. Anisotropic Fluctuations in the Ordered Phases

A rigorous approach for studying anisotropic fluctuations based on the exact self-consistent solutions has been developed by Shi et al.[19] Here, we provide a simpler, approximate approach based on an order-parameter free energy functional. Although not accurate enough for quantitative purposes, the current approach is much simpler to implement and is mathematically more transparent than the rigorous one. Since the issues addressed in this paper do not depend on quantitative accuracy, we choose this simpler approach.

We start with the standard Leibler free energy functional[2] for incompressible diblock copolymers:

$$F[\psi(\vec{k})] = \frac{1}{2}\int d\vec{k}\ \Gamma_2(\vec{k},-\vec{k})\ \psi(\vec{k})\ \psi(-\vec{k}) + \frac{1}{3!}\int d(\vec{k}_1\vec{k}_2)\ \Gamma_3(\vec{k}_1,\vec{k}_2,-\vec{k}_1-\vec{k}_2)\ \psi(\vec{k}_1)\ \psi(\vec{k}_2) \times \psi(-\vec{k}_1-\vec{k}_2) + \frac{1}{4!}\int d(\vec{k}_1\vec{k}_2\vec{k}_3) \times \Gamma_4(\vec{k}_1,\vec{k}_2,\vec{k}_3,-\vec{k}_1-\vec{k}_2-\vec{k}_3)\ \psi(\vec{k}_1)\ \psi(\vec{k}_2)\ \psi(\vec{k}_3) \times \psi(-\vec{k}_1-\vec{k}_2-\vec{k}_3) \quad (1)$$

In the above equation, $\psi(\vec{k}) = \rho_A(\vec{k}) - f$ is the order parameter where $\rho_A(\vec{k})$ is the Fourier transform of the local density of A-monomers and f is the global fraction of the A-block. $\Gamma_2(\vec{k}_1,\vec{k}_2)$, $\Gamma_3(\vec{k}_1,\vec{k}_2,\vec{k}_3)$, and $\Gamma_4(\vec{k}_1,\vec{k}_2,\vec{k}_3,\vec{k}_4)$ are, in general, wavevector-dependent coefficients in the expansion (called the two-point, three-point, and four-point vertex functions, respectively, in the field-theoretical jargon). The two-point vertex function has the form of $\Gamma_2(k,-k) = S_0^{-1}(k) - 2N\chi$, where N is the degree of polymerization, χ is the Flory−Huggins parameter, and $S_0(k)$ is the structure factor for a noninteracting diblock copolymer and is peaked at a wavenumber k^*. In the weak-segregation regime, the density waves are dominated by wavevectors with the optimal wavenumber k^*. Thus we approximate the functions $\Gamma_3(\vec{k}_1,\vec{k}_2,\vec{k}_3)$ and $\Gamma_4(\vec{k}_1,\vec{k}_2,\vec{k}_3,\vec{k}_4)$ by their values corresponding to wavevectors having the optimal magnitude k^*. In this approximation, $\Gamma_3(\vec{k}_1,\vec{k}_2,\vec{k}_3)$ becomes independent of the wavevectors while $\Gamma_4(\vec{k}_1,\vec{k}_2,\vec{k}_3,\vec{k}_4)$ has only a weak angular dependence. We further ignore the angular dependence in Γ_4 by the approximation $\Gamma_4(\vec{k}_1,\vec{k}_2,\vec{k}_3,\vec{k}_4) = \Gamma_4(0,0)$ where $\Gamma_4(0,0)$ is a function defined in ref 2. We denote these functions as γ_3 and γ_4, respectively. These approximations are not necessary and are not expected to have any significant effects on the issue we wish to address in this paper but greatly simplify the calculations and make the results much more transparent. Thus we write the free energy functional as

$$F[\psi(\vec{k})] = \frac{1}{2}\int d\vec{k}\ [S_0^{-1}(k) - 2N\chi]\ \psi(\vec{k})\ \psi(-\vec{k}) + \frac{\gamma_3}{3!}\int d(\vec{k}_1\vec{k}_2)\ \psi(\vec{k}_1)\ \psi(\vec{k}_2)\ \psi(-\vec{k}_1-\vec{k}_2) + \frac{\gamma_4}{4!}\int d(\vec{k}_1\vec{k}_2\vec{k}_3)\ \psi(\vec{k}_1)\ \psi(\vec{k}_2)\ \psi(\vec{k}_3)\ \psi(-\vec{k}_1-\vec{k}_2-\vec{k}_3) \quad (2)$$

$S_0^{-1}(k)$, γ_3, and γ_4 can be calculated easily using standard methods.[2,20] These functions depend on the fraction f of the A-block and on the conformational asymmetry between the two blocks. For simplicity, we shall only address conformationally symmetric diblocks in the rest of the paper, but the general approach developed in this section is equally applicable to conformationally asymmetric cases.

The mean-field order parameter $\psi_0(\vec{k})$ for a given morphology can be written as

$$\psi_0(\vec{k}) = \sum_{\vec{G}} A_{\vec{G}}\,\delta(\vec{k}-\vec{G}) \quad (3)$$

where $\vec{G}$ is the set of reciprocal lattice wavevectors of the morphology and the $A_{\vec{G}}$'s are obtained by minimizing the free energy eq 2 by substituting eq 3 into the free energy.

To study the fluctuation around the mean-field structure, we write

$$\psi(\vec{k}) = \psi_0(\vec{k}) + \delta\psi(\vec{k}) \quad (4)$$

Substituting this into eq 2, keeping terms only up to quadratic order in $\delta\psi(\vec{k})$ and noting the stationary condition for $\psi_0(\vec{k})$, we obtain

$$F[\psi(\vec{k})] = F[\psi_0(\vec{k})] + \frac{1}{2}\int d\vec{k}\ [S_0^{-1}(k) - 2N\chi]\ \delta\psi(\vec{k})\ \delta\psi(-\vec{k}) + \frac{\gamma_3}{2}\sum_{\vec{G}}\int d\vec{k}\ A_{\vec{G}}\,\delta\psi(\vec{k})\ \delta\psi(-\vec{k}-\vec{G}) + \frac{\gamma_4}{4}\sum_{\vec{G}}\sum_{\vec{G}'}\int d\vec{k}\ A_{\vec{G}}A_{\vec{G}'}\,\delta\psi(\vec{k})\ \delta\psi(-\vec{k}-\vec{G}-\vec{G}') \quad (5)$$

The presence of periodic order makes the fluctuations in $\vec{k}$-space nondiagonal. To study the anisotropic fluctuation and the stability of the ordered phases, the quadratic term of free energy needs to be diagonalized. This generally requires diagonalization of a very large matrix. In this work, we make the simplifying approximation that the dominant fluctuation arises from modes with wavevectors $|\vec{k}| \approx k^*$. This approximation is justified in the weak segregation regime where fluctuations are mainly determined by the leading quadratic coefficient $S_0^{-1}(k) - 2N\chi$, which has a minimum at $k = k^*$. Using this approximation, the matrix can be truncated to a smaller matrix involving $\vec{k}$ and $\vec{k} \pm \vec{G}$ and can then be diagonalized analytically; the

eigenvalues of this matrix determine the stability of an ordered structure. The structure is stable or metastable if all the eigenvalues are positive. The spinodal of a structure is reached when the lowest eigenvalue turns negative.

The structure factor of an ordered phase when it is stable or metastable is given by

$$\langle\psi(\vec{k})\,\psi(-\vec{k})\rangle = \psi_0(\vec{k})\,\psi_0(-\vec{k}) + \langle\delta\psi(\vec{k})\,\delta\psi(-\vec{k})\rangle \quad (6)$$

The fluctuation part of the structure factor $\langle\delta\psi(\vec{k})\,\delta\psi(-\vec{k})\rangle$ is obtained by taking the diagonal element of the inverse matrix of eq 5.

III. Precursor of the PL Phase: Anisotropic Fluctuations in the L Phase near Its Spinodal

For the mean-field lamellar structure, we assume a sinusoidal wave in the z-direction for the order parameter, with amplitude A_0 and wavevector $k_z = k^*$ (We ignore the shift of the wavenumber from k^* in this weak segregation regime, although this can be taken into account with little consequence). A_0 is obtained by minimizing the free energy eq 2.

To study the fluctuation spectrum and the stability of the L phase, we consider a small perturbation of the form given by eq 4, as discussed in the last section. The diagonalization of the matrix in eq 5 can be easily performed with the result that the lowest eigenvalues lie on two rings at $k_z = \pm^1/_2 k^*$ and $|\vec{k}| = k^*$. Thus the dominant fluctuations will come from wavevectors on these rings. This result can be easily understood as follows: the calculation of the fluctuation spectrum is mathematically analogous to finding the energy band of nearly free electrons in a weak periodic potential. (The potential in the present case is due to the mean-field sinusoidal lamellar wave. In the weak segregation regime and under the assumption that fluctuations are dominated by wavevectors around $k = k^*$, this potential is dominated by the γ_3-term in eq 5). It is well-known from solid state physics[21] that the energy band develops a gap at the boundary of the first Brillouin zone, which in the case of a lamellar structure corresponds to $k_z = \pm^1/_2 k^*$. This band gap lowers the energy of the electron in the lower band; in the present context, such a band gap decreases the free energy cost for fluctuations at the band edge. However, unlike the case of electrons that have a dispersion relation of the form $\epsilon \sim k^2$ (in the absence of the periodic potential), in the case of diblock copolymers the dispersion relation is rather $\epsilon \sim (k - k^*)^2$. Thus the least costly fluctuations have to be on the surface of the sphere, $|\vec{k}| = k^*$. The intersection of the plane at $k_z = \pm^1/_2 k^*$ with the surface of the sphere $|\vec{k}| = k^*$ is just the two rings indicated in Figure 1.

Thus, as $N\chi$ decreases, the least stable fluctuations occur on the two rings; see Figure 1. The vanishing of the eigenvalue corresponding to these least stable modes, or equivalently, the divergence of the fluctuations of these modes, signals the spinodal of the lamellar structure.

Figure 2 shows the structure factor in the $k_x = 0$ plane of the L phase with $f = 0.35$ in the metastable state near the spinodal. (The two Bragg spots at $k_z = \pm k^*$, $k_y = 0$ due to the mean-field lamellar wave are not shown.) The scattering due to fluctuations at $k_z = \pm^1/_2 k^*$ and $k_y = \pm^{\sqrt{3}}/_2 k^*$ is a result of the intersection of the rings with the $k_x = 0$ plane. The same scattering pattern was obtained earlier by Yeung et al.[17] using a more rigorous approach.

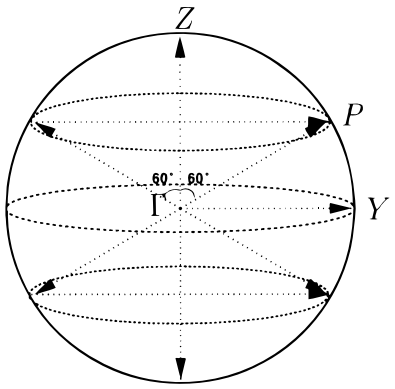

Figure 1. Schematic showing the two rings in the k-space at $k_z = \pm^1/_2 k^*$ corresponding to the least stable fluctuation mode in a lamellar structure of wavevector $k_z = k^*$.

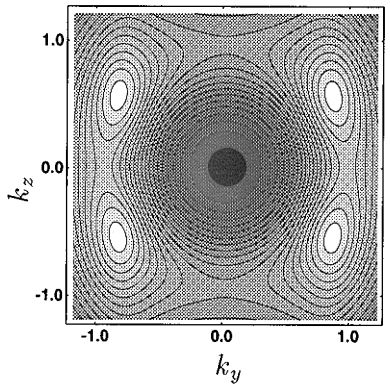

Figure 2. Fluctuation part of the scattering pattern of the L phase with $N\chi = 18.0$ and $f = 0.35$ in the $k_x = 0$ plane in units of k^*. Since the z-axis is the symmetry axis, the three-dimensional pattern is the 2π rotation of this pattern with respect to the z-axis. The two Bragg spots at $k_z = \pm k^*$, $k_y = 0$ due to the mean-field lamellar wave are not shown.

Although the scattering pattern resulting from the linear stability analysis lacks any in-layer structure (in the x, y plane), the finding that the dominant fluctuations occur at $k_z = \pm^1/_2 k^*$ leads to the important conclusion that any structures that form as a result of instability of the L phase will have a periodicity of two layers. Thus the *abab*... stacking model is consistent with this conclusion while the *abcabc*... stacking model is not. In the next section we propose two *abab*... stacking models.

IV. Structure and Stability of the PL Phase

The linear stability analysis in the previous section suggests that the PL phase forms as the least stable mode when the L phase reaches its spinodal. Further evolution of these fluctuations into a three-dimensional structure cannot be predicted by such a linear stability analysis. The question of pattern selection due to nonlinear interactions at present is still not fully resolved[22] and is thus beyond the scope of the present work. However, our time-dependent Ginzburg−Landau simulation of the structural evolution beyond the spinodal of the L phase, shows unambiguously a well-defined *abab*... stacking pattern of perforated layers with clear periodic in-layer structures,[15] although the exact symmetry of the in-layer structures is difficult to ascertain because of the small system size used in the simulation.

Given that the PL phase is a three-dimensional periodic structure that forms out of the least stable

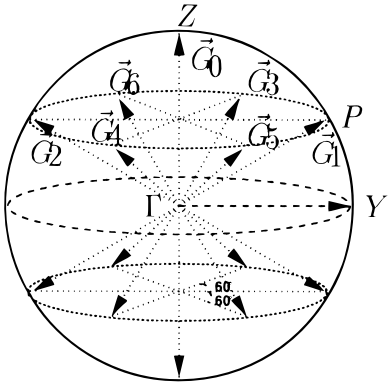

Figure 3. First-order reciprocal lattice wavevectors of a hcp-based PL.

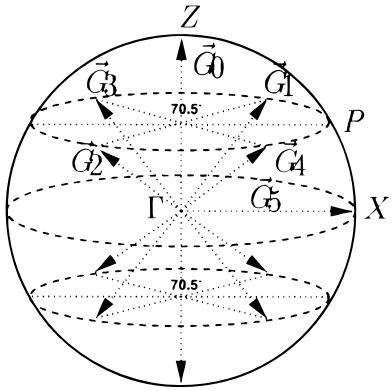

Figure 4. First-order reciprocal lattice wavevectors of a bcc-based PL.

mode of the L phase as discussed in the last section, it follows that the first-order reciprocal lattice points that are responsible for the structure must reside on the two rings shown in Figure 1. Symmetry considerations limit their distribution on the ring to two choices within the simple space group with reflection symmetry.[23] In the first choice, there are six reciprocal lattice points equally spaced on each ring. The in-layer structure thus has hexagonal symmetry. The set of wavevectors for the three-dimensional structure is shown in Figure 3. Note that the differences formed among the six wavevectors $\vec{G}_1 \cdots \vec{G}_6$ give rise to three other sets of wavevectors that lie in the $k_z = 0$ plane, the smallest of which coincide with the projections of $\vec{G}_1$ through $\vec{G}_6$ in that plane. The next two sets are outside the sphere in the figure. Because these wavevectors have magnitudes that are different from k^*, the amplitudes of these waves are quite small and can be neglected for most purposes. We shall name the PL phase of this structure the hcp-based PL.

The second choice has four spots on each ring at $k_z = \pm 1/2 k^*$ and $|\vec{k}| = k^*$. The most symmetric arrangement is into a square; this would give rise to an in-layer square lattice. More generally, the four spots can be arranged into a rectangle. Although symmetry considerations alone are incapable of predicting the angles between these spots, based on the fact that density waves in the weak segregation regime are dominated by those having the optimal wavenumber k^*, we expect that the optimal arrangement will be such that some of the in-plane wavevectors formed by the difference between the four wavevectors $\vec{G}_1$ through $\vec{G}_4$ have a magnitude of k^*. This consideration leads to a reciprocal lattice shown in Figure 4. In the one wavenumber approximation, this reciprocal lattice is that of the bcc

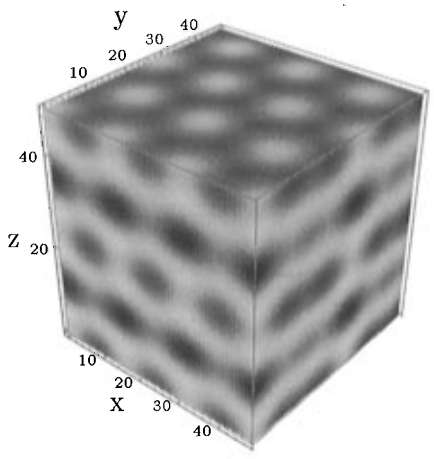

(a) hcp-based PL phase

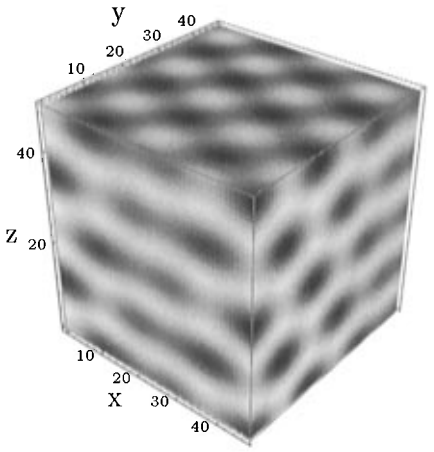

(b) bcc-based PL phase

Figure 5. Microstructure generated using the wavevectors in (a) Figure 3 and (b) Figure 4. The wave amplitudes are obtained at the stationary point of the corresponding PL phase.

structure. Thus we name the PL phase of this structure the bcc-based PL.

The real space structure of the PL phase corresponding to the two reciprocal-space structures in Figures 3 and 4 are shown in Figure 5a,b; both structures have the *abab*... stacking.

Using the representation of the PL structure in Figures 3 and 4, we have calculated the stability of the two PL models using the free energy functional, eq 2. Within the framework of this free energy, we find that neither the hcp-based nor the bcc-based PL is the lowest free energy state when compared with the L, G, H, and BCC phases. However, they can exist as metastable states in the region of the phase diagram where the G phase is thermodynamically stable. The bcc-based PL phase has a slightly lower free energy than the hcp-based PL phase, but given the approximations in the theory, such a small difference should not be taken to be of significance. At smaller $N\chi$ and/or f, the PL structure loses its local stability characterized by one or more of the eigenvalues of the matrix turning negative. It should be pointed out that because of the multidimensionality of the order parameter (due to the multitude of the reciprocal lattice wavevectors), some eigenvalues remain positive. Therefore, in general, the

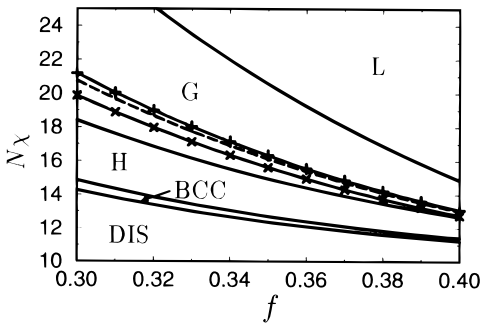

Figure 6. Phase diagram for a conformationally symmetric diblock copolymer system. The solid lines are conventional phase boundaries for L, G, H, BCC, and DIS (the disordered phase); the long dashed line is the spinodal line for L; the dotted line with "+" is the spinodal line for the metastable hcp-based PL, while the dotted line with "x" is the spinodal line for the metastable bcc-based PL.

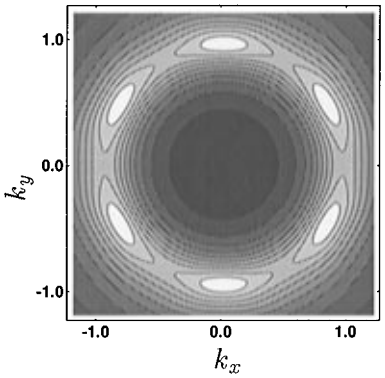

Figure 7. Fluctuation part of the scattering pattern in the $k_z = 0$ plane for a metastable hcp-based PL. The parameters are chosen at $N\chi = 17$ and $f = 0.35$.

structure beyond the spinodal limit corresponds to a saddle point in the free energy surface, which we termed pseudostable structure in our previous work.[15] We comment here that allowing $\vec{G}$ to be different from k^* will generally lead to a lower free energy and a slight modification of the structure. However, the effect is quantitative rather than qualitative, and in the weak segregation regime, the effect is negligible.

The high-temperature spinodals of the two PL structures are shown in a restricted part of the phase diagram in Figure 6. Shown there also is the spinodal of the L phase. These three spinodal lines are quite close. Given the approximations in the theory, their relative position in the phase diagram is probably not very meaningful. That they are quite close, however, is significant in understanding the experimental conditions that produce the observed PL structures, as will be discussed in section V.

In the metastable PL state, it is meaningful to define a (quasi)equilibrium structure factor. The procedure for calculating the fluctuation part of the structure factor is described in section II. Again, for simplicity of calculation, we assume that the dominant fluctuations arise from modes with wavevectors $|\vec{k}| \approx k^*$, although higher order reciprocal lattice wavevectors are used in the representation of the structure as well as in the calculation of the free energy.

Of particular interest is the in-layer scattering pattern (the intensity plot of the structure factor in the $k_z = 0$ plane). Figure 7 shows the fluctuation part of the scattering pattern for the hcp-based PL for a diblock

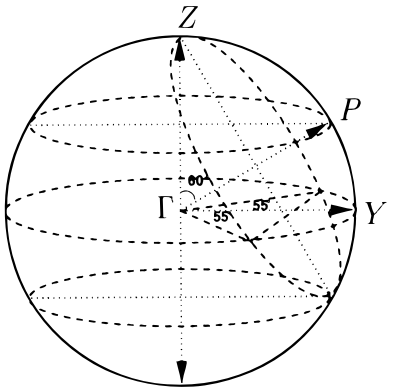

Figure 8. Geometric construction for obtaining the locations of the strongest scattering spots in the $k_z = 0$ plane.

with $f = 0.35$ and $N\chi = 17$. The 6-fold symmetry compares well with the SANS pattern obtained by Bates and co-workers.[4,11] Though not obvious from the figure, each peak in Figure 7 is actually a combination of two peaks positioned 10° apart. Thus the combined peak has a rather wide angular spread. The positions of the two peaks can be understood by the same geometric construction used to understand the fluctuation spectrum in the L phase. For each of the 12 wavevectors ($\vec{G}_1$ through $\vec{G}_6$ and their inverse) we form a plane perpendicular to the wavevector by cutting through the middle of the vector. The intersection of this plane with the sphere $k = k^*$ forms a ring. The intersection of this ring with the scattering plane (in this case the $k_z = 0$ plane) yields the peak positions of the scattering intensity due to fluctuation. This is illustrated in Figure 8. Note that each wavevector is responsible for two scattering spots in the $k_z = 0$ plane. Thus the six wavevectors $\vec{G}_1$ through $\vec{G}_6$ yield 12 scattering spots in the $k_z = 0$ plane. The inverse vectors of $\vec{G}_1$ through $\vec{G}_6$ lead to scattering spots in the $k_z = 0$ plane that are identical in their location to the 12 spots from $\vec{G}_1$ through $\vec{G}_6$. Therefore, this construction leads to 12 distinct points on the ring at $k_z = 0$ and $|\vec{k}| = k^*$. Strictly speaking, the above geometric procedure is valid for weak sinusoidal periodic potentials. In the metastable PL state, the amplitude of the order parameters is not very small; also there are now higher order harmonics contributions. These effects lead to the result that the peaks shift slightly inward from the ring at $|\vec{k}| = k^*$, as shown in Figure 7.

The scattering pattern in Figure 7 shows only contributions due to fluctuation in the order parameter. The full scattering function includes also contributions due to Bragg scattering from six in-plane wavevectors that are formed from the difference between two adjacent wavevectors in the set $\vec{G}_1$ through $\vec{G}_6$. The six spots are at the same angular position as the six peaks in Figure 7, but at a distance $\sqrt{3}/2 k^*$ from the origin. Because of the weakness of these Bragg peaks and the unavoidable broadening of Bragg peaks in the experiments, these peaks will be combined with the scattering peaks due to fluctuation to give the appearance of six broad peaks with the apparent peak position somewhere between $0.866\,k^*$ and k^*. This is in excellent agreement with experiment.[4,11,24]

The fluctuation part of the scattering function for the bcc-based PL can be obtained in a similar manner, with the resulting scattering pattern shown in Figure 9. Note now that the six scattering peaks are no longer

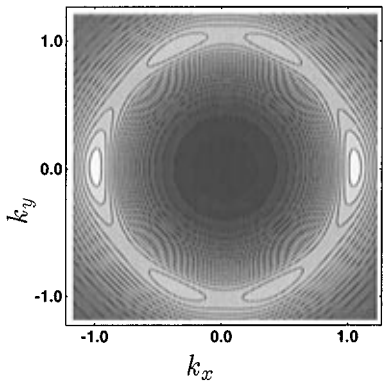

Figure 9. Fluctuation part of the scattering pattern in the $k_z = 0$ plane for a metastable bcc-based PL. The parameters are chosen at $N\chi = 17$ and $f = 0.35$.

6-fold symmetric. The two peaks at $k_x = 0$ are much stronger than the other four. The four weak peaks are situated at angles 19.47° from the k_x axis, on the ring $|\bar{k}| = k^*$. In addition to the six scattering peaks due to fluctuation, there are also two Bragg spots (not shown in the figure) from the mean-field structure that are located at the same positions at the two bright spots; thus the total scattering intensity at the two bright spots will be even stronger.

The scattering pattern Figure 9 was observed in the work of Förster et al.[10] These authors attributed the scattering pattern as arising from perforated layers with *abcabc*... stacking with the layer normal in the *x*-direction. Although capable of accounting for the location of the four weak peaks, their model would predict, as noted by these authors, two additional Bragg peaks in the $k_z = 0$ plane at ±35.26° with respect to the *x*-axis, which were not observed in their SANS pattern. Also, the weakness of the four weak peaks was never satisfactorily explained. Our model based on anisotropic fluctuation in a bcc-based PL, on the other hand, predicts the correct position of all the peaks observed in the experiment. The predicted disparity in the intensity between the two groups of peaks is also in excellent qualitative agreement with experiments. As pointed out at the end of section III, if we assume that the PL phase results from the least stable fluctuation mode of the L phase, then the perforations will be stacked in the *abab*... pattern. Our bcc-based PL model satisfies this requirement and gives a fully consistent explanation of all the features observed in the puzzling SANS data.

V. Discussion

In this paper, we have proposed a consistent theoretical explanation of the nature of the perforated layer (PL) phases that were experimentally observed for a number of diblock copolymer samples. Arguing that the PL phase arises from the least stable fluctuation mode of the lamellar (L) phase, we proposed two structural models for the PL phase, an hcp-based PL and a bcc-based PL, both having *abab*... stacking. Within a Leibler-type mean-field theory, we find that these structures are not thermodynamically stable phases but are only pseudostable in the weak segregation limit and metastable in the intermediate segregation regime. This last conclusion is consistent with more recent experiments by Hajduk et al.[25]

Perhaps the most significant result of this study is a consistent interpretation of the in-plane small-angle neutron scattering patterns for the PL phases obtained by Bates and co-workers.[4,7,10,11,26] Whereas previous attempts have tried to explain the peaks in the scattering patterns in terms of the crystal symmetry of the reciprocal lattice of the structure, i.e., as Bragg scattering, we propose that the experimentally observed scattering peaks arise from anisotropic fluctuations instead of, and in some cases in addition to, Bragg scattering from the mean-field periodic structure. Our calculated scattering patterns using the two structural models are in excellent agreement with the experimental data. The weakness of some of these in-plane scattering peaks can be explained by the fact that these peaks are not the primary Bragg peaks associated with the structures but are either peaks arising from anisotropic fluctuations or secondary Bragg peaks that are generally much weaker in the weak segregation regime. Thus we are able to explain in a simple and consistent manner both the intensity and the location of the in-plane scattering peaks, particularly with regard to the puzzling non-6-fold-symmetric scattering patterns in the work of Förster et al.,[10] which we associate with the bcc-based PL structure.

In contrast to the classical phases (L, C, and BCC) and the bicontinuous G phase, experimentally the PL phases are not easily obtainable by thermal annealing of the samples. Frequently, a combination of temperature change and shear flow is employed to obtain the PL phases.[4,10,11,25] Although the study of shear flow effects is beyond the scope of this work, our results can be used to qualitatively understand the elusiveness of the PL phase in experiments, as explained in the following.

From our calculated phase diagram, the spinodal of the PL phase (for both models) is very close to that of the L phase. Thus, when the L phase becomes unstable as $N\chi$ decreases (or as the temperature increases), so does the PL phase. If we assume, as we did in this paper, that the PL phase arises from the least stable fluctuation mode of the L phase as the L phase reaches its spinodal, then one cannot obtain a (meta)stable PL by increasing the temperature. Increasing the temperature beyond the spinodal of the L phase results in a pseudostable PL that should subsequently decay to the stable H phase through a continuous symmetry breaking with no change in the reciprocal lattice structure. This is in agreement with our previous computer simulation study of the kinetic pathway of the L to C transitions,[15] and also in agreement with experiments.[4,25] However, a metastable PL phase can be obtained by quenching the temperature from the pseudostable PL.[27] This offers a plausible explanation as to why shear is often used in obtaining a (meta)stable PL, because shear has the effect of decreasing the fluctuations[28,29] (albeit anisotropically) and thus is similar to decreasing the temperature. Shear may also help select one PL structure from the other PL structure. In the absence of shear, the near degeneracy in the free energy between the hcp-based and bcc-based PL structures may result in both structures being formed in the same sample, thus leading to PL structures with apparently poor spatial order.[25]

The region of metastable PL overlaps with that of the G phase. Thus over a sufficiently long time the metastable PL will anneal to the more stable G phase. However, we find that the mechanism of this transformation cannot be described by some unstable modes of the PL phase. Such a transition likely involves structural rearrangement in real space, based on spacing and

topological requirements. Since both the G phase and the bcc-based PL structure have a cubic underlying lattice, the transition from PL to G is likely to involve the bcc-based rather than the hcp-based PL. We are currently investigating this transition mechanism.

Acknowledgment. We thank F. S. Bates, D. A. Hajduk, and E. L. Thomas for helpful discussions. This research is supported in part by the National Science Foundation (Grant Nos. ASC-9217368 and DMR-9531914), the Camille and Henry Dreyfus Foundation (Award No. TC-96-063), and the Alfred P. Sloan Foundation (Award No. BR-3508).

References and Notes

(1) Bates, F. S.; Fredrickson, G. H. *Annu. Rev. Phys. Chem* **1990**, *41*, 525. Fredrickson, G. H.; Bates, F. S. *Annu. Rev. Mater. Sci* **1996**, *26*, 501 and references therein.
(2) Leibler, L. *Macromolecules* **1980**, *13*, 1602.
(3) Vavasour, J. D.; Whitmore, M. D. *Macromolecules* **1992**, *25*, 5477.
(4) Hamley, I. W.; Koppi, K. A.; Rosedale, J. H.; Bates, F. S.; Almdal, K.; Mortensen, K. *Macromolecules* **1993**, *26*, 5959.
(5) Thomas, E. L.; Anderson, D. M.; Henkee, C. S.; Hoffman, D. *Nature* **1988**, *334*, 598.
(6) Hajduk, D. A.; Harper, P. E.; Gruner, S. M.; Honeker, C. C.; Kim, G.; Thomas, E. L.; Fetters, L. J. *Macromolecules* **1994**, *27*, 4063.
(7) Schulz, M. F.; Bates, F. S.; Almdal, K.; Mortensen, K. *Phys. Rev. Lett.* **1994**, *73*, 86.
(8) Matsen, M. W.; Schick, M. *Phys. Rev. Lett.* **1994**, *72*, 2660.
(9) Matsen, M. W.; Bates, F. S. *Macromolecules* **1996**, *29*, 1091.
(10) Förster, S.; Khandpur, A. K.; Zhao, J.; Bates, F. S.; Hamley, I. W.; Ryan, A. J.; Bras, W. *Macromolecules* **1994**, *27*, 6922.
(11) Khandpur, A. K.; Förster, S.; Bates, F. S.; Hamley, I. W.; Ryan, A. J.; Bras, W.; Almdal, K.; Mortensen, K. *Macromolecules* **1995**, *28*, 8796.
(12) de la Cruz, M. O.; Mayes, A. M.; Swift, B. W. *Macromolecules* **1991**, *25*, 944.
(13) Fredrickson, G. H. *Macromolecules* **1991**, *24*, 3456.
(14) Hamley, I. W.; Bates, F. S. *J. Chem. Phys* **1994**, *100*, 6813.
(15) Qi, S. Y.; Wang, Z.-G. *Phys. Rev. E.* **1997**, *55*, 1682.
(16) Qi, S. Y.; Wang, Z.-G. *Phys. Rev. Lett.* **1996**, *76*, 1679.
(17) Yeung, C.; Shi, A.-C.; Noolandi, J.; Desai, R. C. *Macromol. Theory Simul.* **1996**, *5*, 291.
(18) Laradji, M.; Shi, A.-C.; Desai, R. C.; Noolandi, J. *Phys. Rev. Lett.* **1997**, *78*, 2577; *Macromolecules*, **1997**, *30*, 3242.
(19) Shi, A.-C.; Noolandi, J.; Desai, R. C. *Macromolecules* **1996**, *29*, 6487.
(20) Ohta, T.; Kawasaki, K. *Macromolecules* **1986**, *19*, 2621.
(21) See Kittel, C. *Solid State Physics*; Wiley: New York, 1976.
(22) Cross, M. C.; Hohenberg, P. C. *Rev. Mod. Phys.* **1993**, *65*, 851.
(23) A third and trivial choice has two spots 180° from each other on the ring; this corresponds simply to a hexagonally ordered cylinder phase with the cylinder axis perpendicular to the layer normal of the original L phase.
(24) The predicted wide angular spread of the in-plane scattering peaks is consistent with the experimental data in refs 4 and 11. However, in another paper (Hamley, I. W.; Gehlsen, M. D.; Khandpur, A.K.; Koppi, K. A.; Rosedale, J. H.; Schulz, M. F.; Bates, F. S.; Almdal, K.; Mortensen, K. *J. Phys. II Fr.* **1994**, *4*, 2161) a narrower angular spread for the six peaks was observed. These sharper peaks are probably due to deviation from the weak segregation regime. Such deviation would enhance the secondary Bragg peaks and suppress the anisotropic fluctuations.
(25) Hajduk, D. A.; Takenouchi, H.; Hillmyer, M. A.; Bates, F. S.; Vigild, M. E.; Almdal, K. *Macromolecules* **1997**, *30*, 3788.
(26) Almdal, K.; Koppi, K. A.; Bates, F. S. *Macromolecules* **1993**, *26*, 4058.
(27) Qi, S. Y.; Wang, Z.-G. Unpublished.
(28) Cates M. E.; Milner, S. T. *Phys. Rev. Lett* **1989**, *62*, 1856.
(29) Fredrickson, G. H. *J. Rheol.* **1994**, *38*, 1045.

MA970206T